Applied Surface Science 292 (2014) 488–493

Contents lists available at ScienceDirect

Applied Surface Science

journal homepage: www.elsevier.com/locate/apsusc

Fluorine interaction with defects on graphite surface by a first-principles study

Song Wang[a,d], Xuezhi Ke[b,*], Wei Zhang[a,e], Wenbin Gong[a,d], Ping Huai[a,f], Wenqing Zhang[c], Zhiyuan Zhu[a,e]

[a] Shanghai Institute of Applied Physics, Chinese Academy of Sciences, Shanghai 201800, China
[b] Department of Physics, East China Normal University, Shanghai 200062, China
[c] State Key Laboratory of High Performance Ceramics and Superfine Microstructure, Shanghai Institute of Ceramics, Chinese Academy of Sciences, Shanghai 200050, China
[d] Graduate University of Chinese Academy of Science, Beijing 100049, China
[e] Key Laboratory of Interfacial Physics and Technology, Chinese Academy of Sciences, Shanghai 201800, China
[f] Key Laboratory of Nuclear Radiation and Nuclear Energy Technology, Chinese Academy of Sciences, Shanghai 201800, China

ARTICLE INFO

Article history:
Received 19 July 2013
Received in revised form 1 December 2013
Accepted 1 December 2013
Available online 8 December 2013

Keywords:
Graphite
Diffusion
Reaction
First principles
Molten salt reactor
Fluorine

ABSTRACT

The interaction between fluorine atom and graphite surface has been investigated in the framework of density functional theory. Due to the consideration of molten salt reactor system, only carbon adatoms and vacancies are chemical reactive for fluorine atoms. Fluorine adsorption on carbon adatom will enhance the mobility of carbon adatom. Carbon adatom can also be removed easily from graphite surface in form of CF_2 molecule, explaining the formation mechanism of CF_2 molecule in previous experiment. For the interaction between fluorine and vacancy, we find that fluorine atoms which adsorb at vacancy can hardly escape. Both pristine surface and vacancy are impossible for fluorine to penetrate due to the high penetration barrier. We believe our result is helpful to understand the compatibility between graphite and fluorine molten salt in molten salt reactor system.

1. Introduction

As a result of the increasing consuming of energy, sustainable and renewable energy source becomes more necessary. Nuclear energy is the most important sustainable energy source in future utility. Molten salt reactor (MSR), one of the promising generation IV nuclear reactors, is liquid fuel reactor that used for producing electricity or hydrogen [1]. In this system, the flowing molten salt (LiF, BeF_2) is used as coolant, and graphite is used as neutron moderator. The compatibility of nuclear graphite with flowing molten salt is one of the technology gaps for MSR. Yang et al. [2] investigate the interaction between IG-110 nuclear graphite and molten salts (46.5 mol% LiF, 11.5 mol% NaF, and 42 mol% KF). In the experiment, a huge number of C–F bond are found in products. The behavior of graphite is not satisfactory after two days of immersion of graphite in molten salt at 500 °C [3]. Thus, the fluorine anions play a key role in this system, and it is worth studying the interaction between graphite and fluorine theoretically.

The interaction between fluorine and carbon based materials has been studied for several decades [4–10]. A large number of experiments indicate that graphite can react with fluorine and oxidizing fluorine compounds, resulting in the formation of graphite fluoride CF_x where x is from 0 to 1 depending on the reaction temperature and pressure [7,8,11]. It has been found that CF_x will decompose into gaseous product, including CF_2 molecule, in high temperature [12–14]. Fluorinated carbon nanotube can also decompose into CF_4 molecule at about 800–1200 K [15]. Lee et al. [16] and Tse et al. [17] demonstrate that the successive adsorption of fluorine atom on graphene and carbon nanotube weakens the C–C bond significantly, and eventually the bonds can be broken by pyrolysis. All these studies indicate that graphite fluoride is thermally unstable. However, based on the energetics studies, we find that graphite is stable in MSR system, which consists with the experiment of Oak Ridge National Laboratory [18,19].

This study focuses on the surface reaction in MSR system, which is quite different from previous studies [16,17]. In molten salt system, LiF is in form of Li+ and F−. While, some chemically reactive defects will interact with molten salts, resulting in the formation of F radicals on graphite. Thus, we actually study the interaction between the F radicals and graphite defects. We point out that defects, including carbon adatom and vacancy, are

* Corresponding author. Tel.: +86 21 5571113/+86 21 52711138.
E-mail address: xzke@phy.ecnu.edu.cn (K. Xuezhi).

0169-4332/$ – see front matter © 2013 Elsevier B.V. All rights reserved.
http://dx.doi.org/10.1016/j.apsusc.2013.12.001

Table 1
Convergence tests for different graphite layers. E_{ads} and E_{adsv} are adsorption energy of fluorine atom on pristine surface and vacancy, respectively.

Layers	One layer	Two layers	Four layers
E_{ads} (eV)	−0.87	−0.88	−0.88
E_{adsv} (eV)	−3.98	−4.00	−4.00
CF group diffusion barrier (eV)	0.34	0.35	0.35

chemically reactive to fluorine in MSR. Fluorine atoms could adsorb on carbon adatom, forming CF or CF_2 group. The stable adsorption of fluorine on vacancy explains the formation of C–F bond which has been found in experiment. The high penetration barrier of fluorine atom through graphite surface consists with the experiment that fluorine ion can't penetrate graphite surface even with kinetic energy of 10 eV. Our result explains the compatibility between graphite and molten salt theoretically.

2. Methodology

In this work, all the first-principles calculations are carried out using Vienna *Ab initio* Simulation Package (VASP). Both the local density approximation (LDA) [20] and the generalized gradient approximation (GGA) [21] were used as the exchange-correlation functional in our calculations. The projector augmented wave potential method [22] is used with a plane wave basis set limited by the cutoff energy of 450 eV. The momentum space integration is performed using $2 \times 2 \times 1$ Monkhorst–Pack [23] k-point mesh. The total energy convergence within 2.5 meV per atom was achieved compared with the more dense mesh $4 \times 4 \times 1$ *k*-point. To see the influence of other layers on the adsorption, we have performed a convergence test by using different graphite layers as shown in Table 1. To check the convergence of the fluorine adsorption energy on pristine graphite surface (E_{ads}) and vacancy (E_{adsv}), and diffusion barrier, one-, two- and four-layer graphite surfaces were considered using LDA exchange-correlation functional. Table 1 shows that the two-layer graphite is good enough for our purpose. Thus, most graphite surfaces are modeled as a supercell composed of $5 \times 5 \times 1$ graphite unit cell with periodic boundary condition as illustrated in Fig. 1, which is large enough to simulate the graphite and graphene supercell [24,25]. The $6 \times 6 \times 1$ supercell is used in the study of divacancy. The vacuum slab is 13.0 Å and the second graphene layer is fixed along z direction in all the calculations. It is well-known that the LDA coincidentally yields nearly the correct interlayer spacing for the graphite, thus, the results of graphite system were calculated by using the LDA. The one-layer graphite (graphene) is also acceptable for our calculations with the convergence of 0.02 eV per fluorine, thus, all of the results computed in the GGA are obtained from the graphene. In the calculation of structural optimization, the ionic relaxation will be stopped if all the forces are smaller than 10^{-2} eV/Å. The climbing nudged elastic band (cNEB) method [26,27] is employed to calculate the reaction barrier with the force tolerance of 4×10^{-2} eV/Å. The preferential sticking of hydrogen and fluorine atoms on graphene has been studied by many groups, and the spin density is important for both fluorine and hydrogen sticking [28,29]. However, in our study, the preferential adsorption is related to the dangling bond of defects, which is much stronger than the spin effect. Thus, the spin polarization is not considered in our calculations.

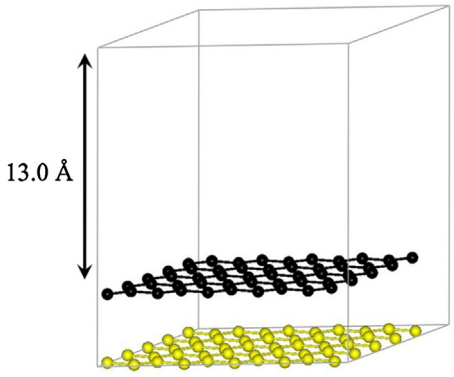

Fig. 1. Supercell model used in our simulations. Black balls are the carbon atoms that can relaxed in three directions, while, yellow balls are carbon atoms fixed in *Z*-axis. (For interpretation of the references to color in this figure legend, the reader is referred to the web version of this article.)

3. Results and discussion

3.1. Interaction between fluorine atoms and carbon adatom

For the pristine graphite surface, the adsorption energy of fluorine atom on graphite surface is calculated to be −0.88 eV (−0.55 eV in the GGA) according to the following equation:

$$E_{ads} = E_{G+F} - E_G - \frac{1}{2}E_{F_2}$$

where E_{G+F}, E_G and E_{F_2} are the total energy of the graphite with fluorine adsorption, total energy of the graphite, and the total energy of an isolated F_2 molecule, respectively. Considering the existence of LiF molecule in the environment of MSR system, we also calculate the formation energy of LiF molecule with respect to Li crystal and F_2 molecule by using following equation:

$$E_{\text{Formation}} = E_{\text{LiF}} - E_{\text{Li}} - \frac{1}{2}E_{F_2}$$

The calculated formation energy for the LiF is −3.32 eV with LDA. This energy is much lower than the energy (−0.88 eV) for fluorine adsorption on the graphite, indicating that in the MSR system it is almost impossible for the fluorine to adsorb on the graphite surface.

The adsorption energy for fluorine atom on the carbon adatom is calculated according to the following equation:

$$E_{\text{ads}} = E_{G+C+G} - E_{G+C} - \frac{1}{2}E_{F_2}$$

where E_{G+C+F} and E_{G+C} are the total energy of graphite with the CF group adsorption and total energy of graphite with the adatom, respectively. The calculated adsorption energy is −4.00 eV (−3.61 eV in the GGA). This energy is lower than the formation energy −3.32 eV of the LiF molecule, indicating that the fluorine prefers to adsorb on the adatom forming CF group in the MSR system.

Actually, the CF group has been detected on the graphite surface [30,31] and also in the gaseous decomposition product of graphite fluoride [13]. It is interesting to see how the CF group diffuses on the surface. Due to the symmetry, the two different diffusion paths are identified for the CF group, i.e., path A and path B, denoted on the top panel of Fig. 2. In path A, the CF group diffuses to the neighboring bridge site within the same hexagon, and in path B, the CF group diffuses to the neighboring bridge site of another hexagon. The corresponding energy profile for path A and path B are shown on the bottom panel of Fig. 2. The diffusion barriers for path A and path B are 0.43 eV and 0.35 eV (0.23 and 0.18 eV in the GGA), respectively. Compared with the pure carbon adatom diffusion barrier of 0.52 eV [32] (in the GGA) these barriers are much lower. Therefore, the fluorine adsorption on the adatom can enhance the mobility of the carbon adatom.

It is also interesting to see how the CF group separates from the graphite surface. The energy profile for the separation is presented in Fig. 3. Fig. 3 shows that the energy profile for the process

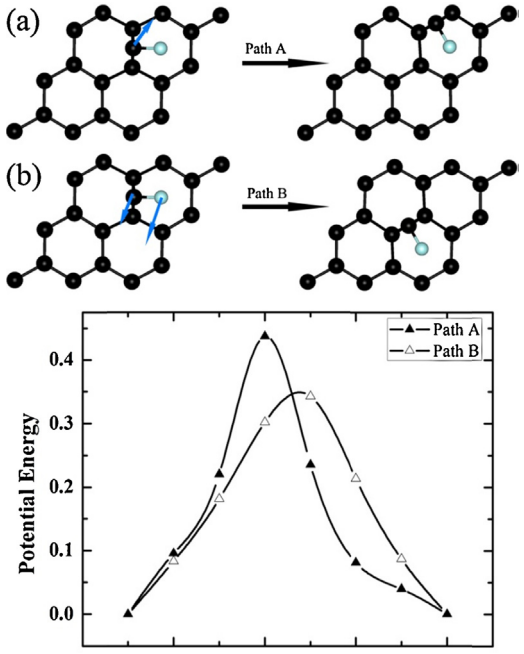

Fig. 2. Top panel: The CF group diffuses on graphite surface along two reaction paths, denoted as Path A, and Path B. Blue arrows indicate the diffusion directions. Bottom panel: The corresponding energy profile along these two diffusion paths. (For interpretation of the references to color in this figure legend, the reader is referred to the web version of this article.)

increases monotonously with the separation distance. The barrier for the separation is about 0.65 eV (0.35 eV in the GGA). Considering that the working temperature in the MSR system is around 1000 K, this barrier is not high, and hence this separation process could happen.

Considering that the CF group may attract another fluorine atom to form the CF_2 group, we have also investigated the reaction process that the CF_2 separates from the surface. This process is demonstrated as the snapshots on the top panel of Fig. 4, and the corresponding energy profile for the process is shown on the bottom panel of Fig. 4. It can be seen from Fig. 4 that the barrier for the separation is 0.92 eV (0.80 eV in the GGA), this process may still happen in the MSR system. Actually, the decomposition process for fluorinated graphite has been studied by several experimental groups and the product CF_2 has been obtained at

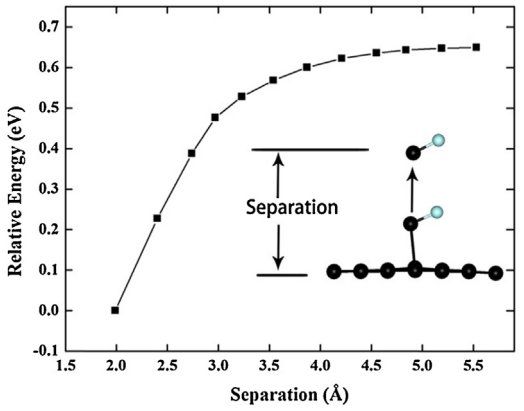

Fig. 3. The relative energy for the reaction process that the CF group separates from the graphite surface (as a function of separation distance). The inset picture denotes the atomic configuration for the initial state and the final state. (For interpretation of the references to color in this figure legend, the reader is referred to the web version of this article.)

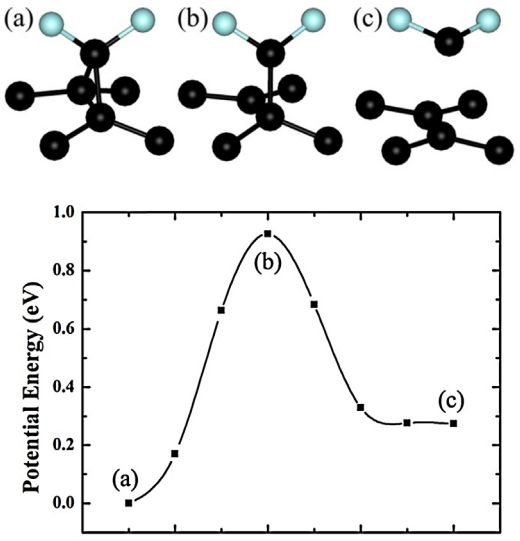

Fig. 4. Top panel: Snapshots for the process that the CF_2 group separates from graphite surface, in which (a) is the initial state, (b) is the saddle point, and (c) is the final state. Bottom panel: The corresponding energy profile for this separation process. (For interpretation of the references to color in this figure legend, the reader is referred to the web version of this article.)

temperature ~700–900 K [12,13,14], and the formation mechanism of CF_2 molecule is not clear. Our current study indicates that the carbon adatom contributes to the product of CF_2.

3.2. Interaction between fluorine and graphite surface with a vacancy

Vacancy is one of typical defects in graphite and graphene [33]. The graphite surface with a vacancy is shown in Fig. 5. According to the symmetry, there are mainly five different adsorption sites around the vacancy which is labeled as the numbers 1, 2, 3, 4 and 5 in Fig. 5. First, let us place one fluorine atom on one of the five sites, and the corresponding adsorption energy is shown in the first line of Table 2. The calculated adsorption energy −0.93 eV at the site 5 is close to that −0.88 eV for the fluorine adsorption on the pristine surface. The adsorption energy for the fluorine at the site 1 is −4.00 eV, which is much more favorable than other sites. This is understandable because the site 1 has a dangling bond, and thus it is more reactive than the other carbon atoms. Considering that the formation energy is −3.32 eV for the LiF, this means that in the MSR system the fluorine prefers to adsorb on the site 1 rather than the other sites of the vacancy. Next, we consider putting one more fluorine atom on one of the five sites in addition to the adsorption of the first fluorine at the site 1. The adsorption energy for the second fluorine is shown in the second line of Table 2. The table shows that the site 1 is still the most stable position for the second fluorine. Then, we continue to put one more fluorine atom to the surface

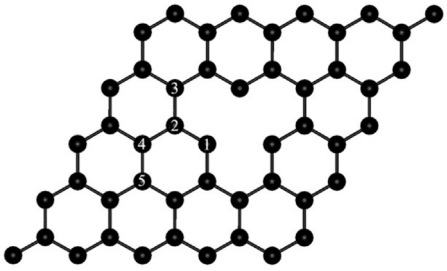

Fig. 5. Five adsorption sites for fluorine around the vacancy are labeled by the numbers 1, 2, 3, 4 and 5.

Table 2
Adsorption energy for fluorine adsorbed at the five different sites of the graphite surface. The positions for site 1, site 2, site 3, site 4, and site 5 are denoted in Fig.5.

Numbers of fluorine atoms	E_{ads} (eV) at				
	Site1	Site2	Site3	Site4	Site5
First fluorine atom	−4.00	−0.98	−1.67	−1.25	−0.93
Second fluorine atom	−2.26	−1.02	−1.78	−1.02	−0.89
Third fluorine atom	–	−1.06	−1.27	−0.85	−1.27

after the two fluorine atoms are adsorbed at the site 1, and the adsorption energy is shown in the third line of Table 2.

It should be mentioned that there are two kinds of single vacancy in experiment: one is the symmetric vacancy, depicted in Fig. 5, and the other is the asymmetric vacancy, which exhibits a Jahn–Teller distortion [34]. The Jahn–Teller distortion, reconstructing into a pentagon ring and nine-membered ring, removes two of the three dangling bonds from the vacancy. Theoretical studies show that Jahn–Teller distortion appears in relatively large supercell, containing 200 atoms [24,34,35]. In our $5 \times 5 \times 1$ supercell, the strains between two neighboring images prevents the reconstruction, meaning that the Jahn–Teller distortion is not found. However, the adsorption of fluorine atoms can also induce the reconstruction of vacancy, reducing the distance between the two edge atoms from 2.46 Å to 1.91 Å, as depicted in Fig. 6(a). This reconstruction lowers the total energy of the system, which is similar to Jahn–Teller distortion.

According to the preceding discussion, the site 1 is the most favorable position for the fluorine atoms, and the other sites are at least 2 eV less favorable than the site 1, indicating that the diffusion from the site 1 to the other sites is extremely difficult (at least 2 eV barrier). For the reaction between the fluorine atoms and the vacancy, one possible process is that carbon atom of site 1 is directly dragged out by one or two fluorine atoms. But this is proved to be extremely difficult since the energy barrier is more than 10 eV and 4.2 eV if carbon atom is dragged out by one or two fluorine atoms, respectively.

In order to obtain a low energy reaction barrier, we figure out a path in which the final state (forming CF_4) is energetically 2.13 eV more favorable than the initial state. The reaction process is demonstrated by the snapshots on the top panel of Fig. 6. During the process one carbon atom at the site 1 is dragged out of the surface, and the reaction product CF_4 molecule is formed and separated from the surface, in which the (a) is the initial state, and the (e) is the final state. The corresponding energy profile for this process is shown on the bottom panel of Fig. 6. During the reaction, the snapshots (a), (b) and (c) demonstrate that one carbon atom is dragged out of the surface by two fluorine atoms (energy barrier 1.79 eV), and the CF_3 group is formed on the surface (the energy drops about

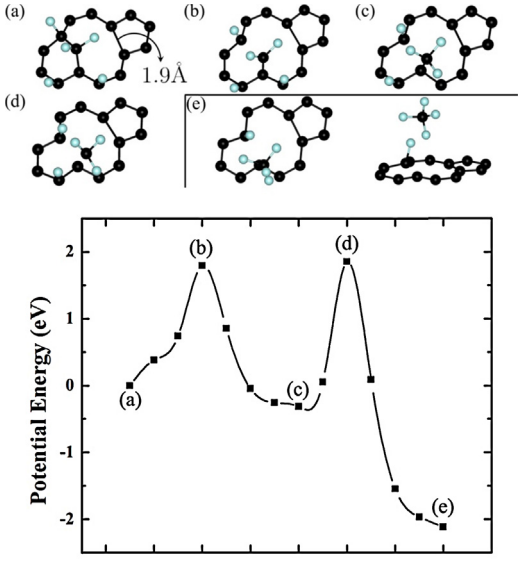

Fig. 6. Top panel: Snapshots for the reaction process between fluorine and graphite surface with a vacancy, in which the (a) is the initial state, the (b) and the (d) are the transition states, the (c) is the local minimum, and the (e) is the final state. The final state (e) has two pictures from two different views. Bottom panel: The corresponding energy profile along the reaction path. (For interpretation of the references to color in this figure legend, the reader is referred to the web version of this article.)

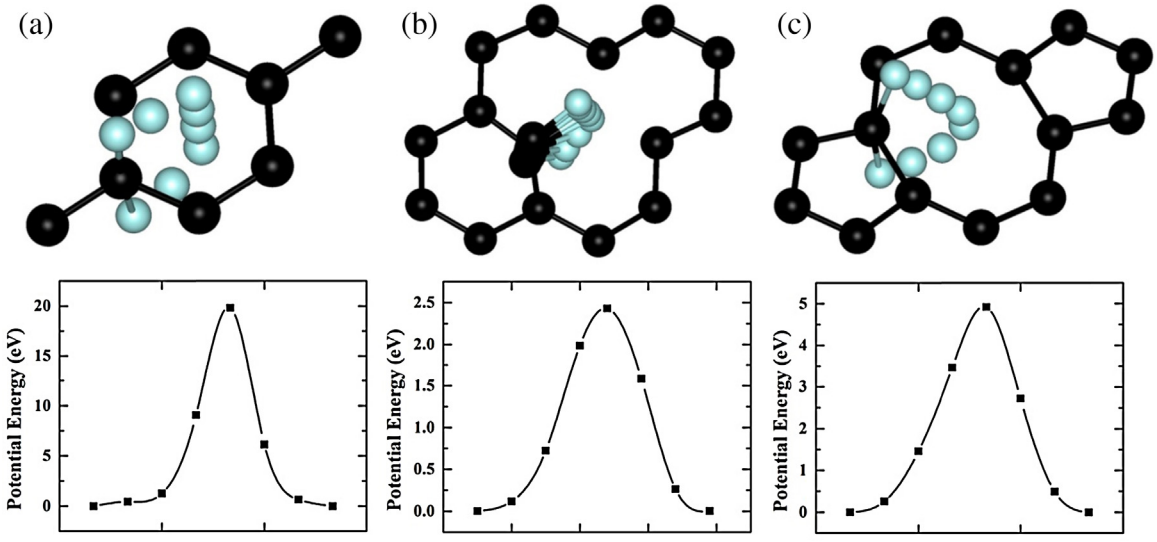

Fig. 7. Top panel: Trajectories for fluorine diffusion through graphite surfaces, in which (a) is the diffusion through the pristine surface, (b) is the diffusion through the surface with a vacancy, and (c) is the diffusion through the surface with a divacancy. Bottom panel: The corresponding energy profile along these diffusion paths for the three types of surfaces. (For interpretation of the references to color in this figure legend, the reader is referred to the web version of this article.)

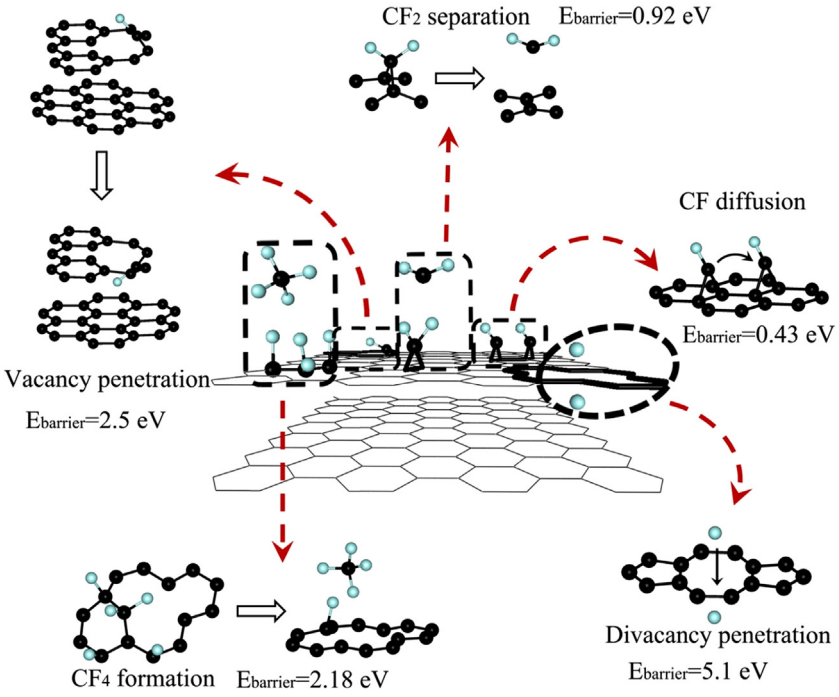

Fig. 8. Schematic diagram for fluorine diffusion and reaction on graphite surfaces. (For interpretation of the references to color in this figure legend, the reader is referred to the web version of this article.)

0.42 eV with the reference to the (a)). The snapshots (c), (d) and (e) demonstrate that the CF_4 molecule is formed from the combination of the CF_3 group and one fluorine atom, after overcoming an energy barrier of 2.18 eV. The two large barriers indicate that this process can rarely happen at low temperature. According to the above study, we conclude that the fluorine is difficult to escape once it is adsorbed at the vacancy. As the experiment [15] indicates, CF_4 molecule is the main product in the decomposition of fluorinated carbon nanotube. This reaction would be considered to be one of the possible procedures of forming CF_4 molecule.

3.3. *Fluorine penetration through graphite surfaces*

It is worth seeing how possibly a fluorine atom penetrates through graphite surface since the intercalated fluorine atom can affect the stability of graphite. Three types of surfaces are considered: pristine surface, surface with a vacancy and surface with a divacancy. The trajectories for fluorine penetration through the three surfaces are demonstrated in the top panel of Fig. 7. At the initial state the fluorine adsorbs on the surface, and at the final state the fluorine atom is located at the graphite interlayer. The corresponding energy profile for the diffusion process is denoted in the bottom panel of Fig. 7. Fig. 7 shows that the penetration barriers for the pristine surface, the vacancy and the divacancy are 20.5 eV, 2.5 eV and 5.1 eV (18.1 eV, 2.0 eV and 4.7 eV in GGA), respectively. The barrier difference can be roughly explained as follows: for the penetration through the vacancy, in Fig. 7(b), the fluorine atom bonds with the carbon atom during the whole process due to the dangling bond. While for the penetration through pristine surface and divacancy, in Fig. 7(a–c), the fluorine atom cannot bond with the carbon during the penetration process. Thus, the diffusion through the vacancy gets the lowest barrier. In the penetration process of pristine surface and divacancy, the repulsive interaction between fluorine atom and carbon atoms determines the penetration barrier. Our calculation reveals that, at the transition state, the distance between the fluorine and the carbon for Fig. 7(a–c) are 1.64 Å and 1.90 Å, respectively. Thus the repulsive interaction through graphite surface is larger than that in divacancy. In a word, the barriers for these processes are quite large, indicating that it is very difficult for the fluorine to penetrate through graphite surfaces. This is consistent with the recent experiments in which the intercalation of molten salt between graphite layers did not occur [3], and fluorine atom with kinetic energy of 10 eV was found to be impossible to pass through graphite surface [36].

4. Conclusion

The interaction between fluorine atoms and defective graphite surface, in molten salt reactor system, has been investigated in the framework of density functional theory. Currently, most of the theoretical and experimental studies concerns on the electronic structures of fluorinated graphene [37,38], in order to realize the utility of fluorinated graphene. Our study focuses on the stability of graphite defects with low fluorine coverage, which is important in molten salt reactor. Comparing the formation energy of LiF molecule and the adsorption energy of fluorine atom at different graphite surfaces structure, including graphite surface, carbon adatom and vacancy, we find that fluorine atoms prefer to adsorb at carbon adatom and vacancy. Due to the adsorption of fluorine atom, the mobility of carbon adatom is enhanced. Carbon adatom can be also removed from graphite surface in the form of CF_2 molecule, which explains the formation mechanism of CF_2 in experiment. After adsorbing fluorine atoms, vacancy is still stable in high temperature. This indicates that graphite is stable even in high temperature molten salt, which consists with the experiment results of Oak Ridge National Laboratory. The penetration barrier of fluorine atom into interlayer through different surfaces infers that fluorine atom can't penetrate graphite surface even in high temperature, which also consists with previous experimental study. Schematic diagram is shown in Fig. 8, which summarizes most of the results in our work.

On the basis of the obtained information, we can discuss the possible processes between the fluorine and graphite in the MSR system. For the perfect graphite, the surface could not adsorb fluorine

atoms, in other words, the graphite surface is compatible with the molten salt in the MSR system, which is consistent with the studies of Oak Ridge National Laboratory. In the MSR, we should take the neutrons emitted from U-235 fission into account. The kinetic energy for the neutrons is around 1 MeV. We can imagine that such a high energy can kick some of the carbons away forming the carbon adatoms and vacancies on the surface. For the adatom surface, the fluoride can easily adsorb on the adatom and this adsorption can enhance the mobility of the adatom, which may lead two possible results: one is that the CF group may escape from the surface, and another is that the high mobility is an advantage for the adatom to repair the vacancy (the latter has low energy). The CF_2 group is also likely to be formed on the surface. If the CF_2 is formed and escapes from the surface, this could be one of the harmful factors for the MSR system. For the surface with a vacancy, the fluorine is difficult to escape once it is adsorbed at the vacancy. This is consistent with the recent experiment by Yang et al. [2]. In the MSR system, the fluorine can hardly penetrate through the surface. This is consistent with the recent experiment by Bernardet et al. [3] in which the intercalation of molten salt between graphite layers was not found.

Acknowledgment

This work is supported by the National Basic Research Program of China (Grant NO. 2010CB934504), Strategic Priority Research Program of the Chinese Academy of Sciences (Grant NO. XDA02040100), National Natural Science Foundation of China (11075196, 11005142, 11074074), and the CAS Hundred Talents Program. We also acknowledge the Shanghai Supercomputer Center for providing computing resources.

References

[1] U.S. DOE, A Technology Roadmap for Generation IV Nuclear Energy Systems, Report USDOE/GIC 002-000, The U.S. DOE Nuclear Research Advisory Committee and the Generation IV International Forum, 2002.
[2] X. Yang, S. Feng, X. Zhou, H. Xu, T.K. Sham, Interaction between nuclear graphite and molten fluoride salts: a synchrotron radiation study of the substitution of graphitic hydrogen by fluoride ion, J. Phys. Chem. A 116 (2011) 985–990.
[3] V. Bernardet, S. Gomes, S. Delpeux, M. Dubois, K. Guérin, D. Avignant, G. Renaudin, L. Duclaux, Protection of nuclear graphite toward fluoride molten salt by glassy carbon deposit, J. Nucl. Mater. 384 (2009) 292–302.
[4] Y. Sato, K. Itoh, R. Hagiwara, T. Fukunaga, Y. Ito, Short-range structures of poly(dicarbon monofluoride) $(CF_2)(n)$ and poly(carbon monofluoride) $(CF)(n)$, Carbon 42 (2004) 2897–2903.
[5] O. Ruff, O. Bretschneider, The reaction products of the different forms of carbon with fluorine, II (carbon-monofluoride), Z. Anorg. Allg. Chem. 217 (1934) 1–18.
[6] O. Ruff, R. Keim, Carbon 4 flouoride (tetrafluor methane), Z. Anorg. Allg. Chem. 192 (1930) 249–256.
[7] H. Fujimoto, A. Mabuchi, T. Maeda, Y. Matsumura, N. Watanabe, H. Touhara, New fluorine-carbon compound prepared by the direct fluorination of mesophase pitch, Carbon 30 (1992) 851–857.
[8] K. Guerin, J.P. Pinheiro, M. Dubois, Z. Fawal, F. Masin, R. Yazami, A. Hamwi, Systhesis and characterization of highly fluorinated graphite containing sp2 and sp3 carbon, Chem. Mater. 16 (2004) 1786–1792.
[9] W. Zhang, L. Spinelle, M. Dubois, K. Guerin, H. Kharbache, F. Masin, A.P. Kharitonov, A. Hamwi, J. Brunet, C. Varenne, A. Pauly, P. Thomas, D. Himmel, J.L. Mansot, New synthesis methods for fluorinated carbon nanofibres and applications, J. Fluorine Chem. 131 (2010) 676–683.
[10] Y. Sato, K. Itoh, R. Hagiwara, T. Fukunaga, Y. Ito, On the so-called semi-ionic C–F bond character in fluorine-GIC, Carbon 42 (2004) 3243–3249.
[11] A. Tressaud, E. Durand, C. Labrugère, Surface modification of several carbon-based materials: comparison between CF_4 rf plasma and direct F_2-gas fluorination routes, J. Fluorine Chem. 125 (2004) 1639–1648.
[12] N. Watanabe, S. Koyama, H. Imoto, Thermal decomposition of graphite fluoride. I. Decomposition products of graphite fluoride, $(CF)_n$ in a vacuum, Bull. Chem. Soc. Jpn. 53 (1980) 2731–2734.
[13] F. Moguet, S. Bordere, A. Tressaud, F. Rouquerol, P. Llewellyn, Deintercalation process of fluorinated carbon fibres—II. Kinetic study and reaction mechanisms, Carbon 36 (1998) 1199–1205.
[14] Y. Sato, R. Hagiwara, Y. Ito, Thermal decomposition mechanism of fluorine–graphite intercalation compounds, Carbon 39 (2001) 951–956.
[15] Z. Gu, H. Peng, R.H. Hauge, R.E. Smalley, J.L. Margrave, Cutting single-wall carbon nanotubes through fluorination, Nano Lett. 2 (2002) 1009–1013.
[16] K. Park, Y. Choi, Y. Lee, C. Kim, Atomic and electronic structures of fluorinated single-walled carbon nanotubes, Phys. Rev. B: Condens. Matter 68 (2003).
[17] M. Wu, J.S. Tse, J.Z. Jiang, Unzipping of graphene by fluorination, J. Phys. Chem. Lett. 1 (2010) 1394–1397.
[18] C.W. Forsberg, A.A. Feltus, Fuel Requirements for the Advanced High Temperature Reactor Graphite Coated Particle Fuel and Molten Fluoride Salt Coolant, in: Report on Technical Meeting on Current Status and Future Prospects of Gas-Cooled Reactor Fuels, IAEA, 2004.
[19] C.W. Forsberg, Molten Salt Reactor Technology Gaps, in: Report on 2006 International Congress on the Advances in Nuclear Power Plants (ICAPP '06), 2006.
[20] D.M. Ceperley, B.J. Alder, Ground-state of the electron-gas by a stochastic method, Phys. Rev. Lett. 45 (1980) 566–569.
[21] J.P. Perdew, K. Burke, M. Ernzerhof, Generalized gradient approximation made simple, Phys. Rev. Lett. 77 (1996) 3865–3868.
[22] G. Kresse, D. Joubert, From ultrasoft pseudopotentials to the projector augmented-wave method, Phys. Rev. B: Condens. Matter 59 (1999) 1758–1775.
[23] H.J. Monkhorst, J.D. Pack, Special points for brillouin-zone integrations, Phys. Rev. B: Condens. Matter 13 (1976) 5188–5192.
[24] A.V. Krasheninnikov, R.M. Nieminen, Attractive interaction between transition-metal atom impurities and vacancies in graphene: a first-principles study, Theor. Chem. Acc. 129 (2011) 625–630.
[25] F. Banhart, J. Kotakoski, A.V. Krasheninnikov, Structural defects in graphene, ACS Nano 5 (2011) 26–41.
[26] G. Henkelman, B.P. Uberuaga, H. Jonsson, A climbing image nudged elastic band method for finding saddle points and minimum energy paths, J. Chem. Phys. 113 (2000) 9901–9904.
[27] G. Henkelman, H. Jo′nsson, Improved tangent estimate in the nudged elastic band method for finding minimum energy paths and saddle points, J. Chem. Phys. 113 (2000) 9978–9985.
[28] D.W. Boukhvalov, M.I. Katsnelson, Chemical functionalization of graphene with defects, Nano Lett. 8 (2008) 4373–4379.
[29] S. Casolo, O.M. Løvvik, R. Martinazzo, G.F. Tantardini, Understanding adsorption of hydrogen atoms on graphene, J. Chem. Phys. 130 (2009) 054704.
[30] M. Baraket, S.G. Walton, E.H. Lock, J.T. Robinson, F.K. Perkins, The functionalization of graphene using electron-beam generated plasmas, Appl. Phys. Lett. 96 (2010) 231501.
[31] K. Tahara, T. Iwasaki, A. Matsutani, M. Hatano, Effect of radical fluorination on mono- and bi-layer graphene in Ar/F-2 plasma, Appl. Phys. Lett. 101 (2012) 163105.
[32] M.T. Lusk, D.T. Wu, L.D. Carr, Graphene nanoengineering and the inverse Stone–Thrower–Wales defect, Phys. Rev. B: Condens Matter 81 (2010) 155444.
[33] A. Hashimoto, K. Suenaga, A. Gloter, K. Urita, S. Iijima, Direct evidence for atomic defects in graphene layers, Nature 430 (2004) 870–873.
[34] A.W. Robertson, B. Montanari, K. He, C.S. Allen, Y.A. Wu, N.M. Harrison, A.I. Kirkland, J.H. Warner, Structural reconstruction of the graphene monovacancy, ACS Nano 7 (2013) 4495–4502.
[35] A.A. El-Barbary, R.H. Telling, C.P. Ewels, M.I. Heggie, P.R. Briddon, Structure and energetics of the vacancy in graphite, Phys. Rev. B: Condens. Matter 68 (2003) 144107.
[36] M. Tagawa, K. Yokota, K. Maeda, A. Yoshigoe, Y. Teraoka, Atomic layer fluorination of highly oriented pyrolytic graphite using hyperthermal atomic fluorine beam, Appl. Phys. Express 2 (2009) 066002.
[37] J.O. Sofo, A.M. Suarez, G. Usaj, P.S. Cornaglia, A.D. Hernández-Nieves, C.A. Balseiro, Electrical control of the chemical bonding of fluorine on graphene, Phys. Rev. B: Condens. Matter 83 (2011) 081411.
[38] S.H. Cheng, K. Zou, F. Okino, H.R. Gutierrez, A. Gupta, N. Shen, P.C. Eklund, J.O. Sofo, J. Zhu, Reversible fluorination of graphene: evidence of a two-dimensional wide bandgap semiconductor, Phys. Rev. B: Condens. Matter 81 (2010) 205435.